

A Neural Network Approach Applied to Multi-Agent Optimal Control

Derek Onken, Levon Nurbekyan, Xingjian Li, Samy Wu Fung, Stanley Osher, and Lars Ruthotto

Abstract—We propose a neural network approach for solving high-dimensional optimal control problems. In particular, we focus on multi-agent control problems with obstacle and collision avoidance. These problems immediately become high-dimensional, even for moderate phase-space dimensions per agent. Our approach fuses the Pontryagin’s Maximum Principle and Hamilton-Jacobi-Bellman (HJB) approaches and parameterizes the value function with a neural network. Our approach yields controls in a feedback form for quick calculation and robustness to moderate disturbances to the system.

We train our model using the objective function and optimality conditions of the control problem. Therefore, our training algorithm neither involves a data generation phase nor solutions from another algorithm. Our model uses empirically effective HJB penalizers for efficient training. By training on a distribution of initial states, we ensure the controls’ optimality is achieved on a large portion of the state-space. Our approach is grid-free and scales efficiently to dimensions where grids become impractical or infeasible. We demonstrate our approach’s effectiveness on a 150-dimensional multi-agent problem with obstacles.

I. INTRODUCTION

Optimal control (OC) problems are ubiquitous in pure and applied mathematics, physics, computer science, engineering, finance, and elsewhere [1], [2], [3]. As a result, theoretical and numerical analyses of OC problems have paramount importance across disciplines. We focus on developing numerical solution methods for general OC problems in high dimensions.

Two of the most common strategies to solve OC problems are Pontryagin’s Maximum Principle (PMP) [4] and the Hamilton-Jacobi-Bellman (HJB) PDE [5] (Sec. II).

PMP is a *local* solution method because optimal controls correspond to fixed initial states. Necessary conditions render an ODE system for the state and *adjoint* variables and a *maximum principle* relating the adjoint variable with the optimal control. This approach is grid-free and thus suitable for high-dimensional problems. However, the aforementioned ODE system is often challenging to solve due to its forward-backward structure [6], [7]. Additionally, the OC problem’s

non-convexity renders the possibility of multiple non-optimal solutions, and additional considerations are necessary, such as the differentiability of the value function [3, Theorem 7.3.9]. Unfortunately, these conditions are virtually impossible to enforce or verify numerically. The effects of non-convexity are especially pronounced in multi-agent collision-avoidance problems [8, I.A]. For OC problems that are convex, high-dimensional solvers can be devised via primal-dual convex optimization methods [9], [10], [11], [12].

Because PMP is a local solution method, disturbances or sudden changes in the system’s initial conditions lead to a new optimization problem. PMP is unattractive for real-time applications because the control-search time is vital.

Alternatively, the HJB approach aims at solving the OC problem for *all initial states at once*. More precisely, the value function—also known as optimal cost-to-go—of an OC problem is a solution of a suitable HJB PDE. After computing the value function, we can recover the optimal control at any state from its gradient. Such controls are said to be in feedback form and are especially useful for real-time applications provided evaluating the feedback form can be done in short calculation-times.

Although effective, HJB equations are challenging to solve numerically, especially when the state’s dimension $d \geq 4$. Firstly, in a deterministic setup, HJB is a first-order non-linear equation and generally does not admit smooth solutions. Secondly, traditional numerical methods for HJB equations, such as ENO/WENO [13], rely on grids and therefore suffer from the curse of dimensionality [5].

We propose a machine learning framework to overcome the curse of dimensionality by approximating the value function with a neural network (NN). Our approach is a fusion of PMP and HJB. Combining the PMP and HJB approaches, we express the control cost in terms of the value function and search for an NN approximation that minimizes this cost on a cloud of initial states. Furthermore, we improve the NN training by adding HJB residual penalties (Fig. 1), similar to [14], [15], [16].

Our approach has several advantages. Firstly, it applies to generic OC problems. Secondly, we find controls in a feedback form that is crucial for real-time applications. Training the NN on a cloud of initial states ensures the controls’ optimality on a large portion of the state-space. Consequently, controls are robust to moderate disturbances or shocks to the system (Fig. 2). Thirdly, our method is grid-free and suitable for high-dimensional problems. Finally, our approach incorporates machine learning techniques for solving large scale optimization problems. As a result, we are able to solve 150-dimensional OC problems (Sec. V-D).

This work was supported in part by NSF award DMS 1751636, AFOSR Grants 20RT0237 & FA9550-18-1-0167, AFOSR MURI FA9550-18-1-0502, Binational Science Foundation Grant 2018209, US DOE, Office of Advanced Scientific Computing Research Field Work Proposal 20-023231, ONR Grants No. N00014-18-1-2527 & N00014-20-1-2093, a gift from UnitedHealth Group R&D, and a GPU donation by NVIDIA Corporation.

D. Onken is with the Department of Computer Science, Emory University, Atlanta, GA, USA (email: donken@emory.edu)

L. Nurbekyan, S. Wu Fung, and S. Osher are with the Department of Mathematics, UCLA, Los Angeles, CA, USA (email: {lnurbek; swufung; sjo}@math.ucla.edu)

X. Li and L. Ruthotto are with the Department of Mathematics, Emory University, Atlanta, GA, USA (email: {xingjian.li; lruthotto}@emory.edu)

Applications of deep learning techniques to OC problems appear in seminal works [17], [18], [19], where the authors apply backward stochastic differential equations techniques to solve high-dimensional stochastic OC problems. In [20], the authors extend these methods by introducing and analyzing different loss functions. These works consider stochastic problems with fixed initial states.

In [21], the authors first generate optimal controls for a sample of initial states then train an NN to fit this data. The data generation phase is performed by a different algorithm [7]. A similar approach exists in [8] with a different data generation algorithm [22].

Our work is based on the same framework as [23], which approximates the feedback control with an NN then optimizes the control cost on a cloud of initial states and provides a theoretical analysis of OC solutions via NN approximations. We extend the framework to finite horizon problems with non-quadratic costs and parameterize the value function instead of the feedback function. This latter approach enables enforcing HJB conditions, which empirically improves numerical performance for solving high-dimensional mean-field games, mean-field control, and normalizing flows [14], [15], [16]. We demonstrate similar advantages in the optimal control problems considered in this work.

We consider deterministic OC problems with a particular emphasis on globally controlling multi-agent systems. For n agents in an q -dimensional space we obtain an $d = n \cdot q$ -dimensional OC problem. Thus, even moderate n, q yield problems that are out of reach for traditional HJB solvers.

We demonstrate the effectiveness of our method by solving a 50-agent control problem in a 3-dimensional space with obstacle and collision avoidance (Fig. 3). The overall dimension of this problem is $d = 150$. Additionally, we demonstrate our model's robustness to shocks and the effect of the penalizers on a 4-dimensional corridor problem.

II. PRELIMINARIES

Here, we briefly recall relevant OC theory. We refer to [1, Chapters I, II] for a detailed exposition. We are interested in deterministic fixed finite time-horizon problems. Consider the time-horizon $[0, T]$ and the system's dynamics given by

$$\partial_s z(s) = f(s, z(s), \mathbf{u}(s)), \quad t \leq s \leq T, \quad z(t) = \mathbf{x}. \quad (1)$$

Here, $\mathbf{z} \in \mathbb{R}^d$ describes the state of the system, and $\mathbf{u} \in U \subset \mathbb{R}^a$ describes the controls. Hence, $f: [0, T] \times \mathbb{R}^d \times U \rightarrow \mathbb{R}^d$ models the evolution of the state $\mathbf{z}: [t, T] \rightarrow \mathbb{R}^d$ in response to the application of a control $\mathbf{u}: [t, T] \rightarrow U$ for initial time $t \in [0, T]$ and initial state \mathbf{x} . We assume that f, L, G, U are sufficiently regular (see [1, Sec. I.3, I.8-9] for a list of assumptions). Next, assume that the control \mathbf{u} yields cost

$$J_{\mathbf{x}, t}[\mathbf{u}] = G(\mathbf{z}(T)) + \int_t^T L(s, \mathbf{z}(s), \mathbf{u}(s)) ds, \quad (2)$$

where $L: [0, T] \times \mathbb{R}^d \times U \rightarrow \mathbb{R}$ is the *running cost* or the *Lagrangian*, and $G: \mathbb{R}^d \rightarrow \mathbb{R}$ is the *terminal cost*. OC problems seek the control that incurs the minimal cost; i.e.,

$$\Phi(t, \mathbf{x}) = \inf_{\mathbf{u}} J_{\mathbf{x}, t}[\mathbf{u}], \quad (3)$$

where Φ is called the *value function*. A solution \mathbf{u}^* of (3) is called an *optimal control*. Accordingly, the \mathbf{z}^* which corresponds to \mathbf{u}^* is called an *optimal trajectory*.

Next, the *Hamiltonian* of the system is given by

$$H(t, \mathbf{x}, \mathbf{p}) = \sup_{\mathbf{u} \in U} \{-\mathbf{p} \cdot f(t, \mathbf{x}, \mathbf{u}) - L(t, \mathbf{x}, \mathbf{u})\}, \quad (4)$$

where we \mathbf{p} is the *adjoint state*. The following is a standing assumption throughout the paper.

Standing Assumption 1: Assume that (4) admits a unique continuous closed-form solution $\mathbf{u}^*(t, \mathbf{x}, \mathbf{p})$.

Under this assumption, one has that

$$L(t, \mathbf{x}, \mathbf{u}^*(t, \mathbf{x}, \mathbf{p})) = \mathbf{p} \cdot \nabla H(t, \mathbf{x}, \mathbf{p}) - H(t, \mathbf{x}, \mathbf{p}). \quad (5)$$

The PMP [4] states that for a solution $(\mathbf{z}^*, \mathbf{u}^*)$ of (3) there exist $\mathbf{p}: [0, T] \rightarrow \mathbb{R}^d$ such that, for $t \leq s \leq T$,

$$\begin{cases} \partial_s \mathbf{z}^*(s) = -\nabla_{\mathbf{p}} H(s, \mathbf{z}^*(s), \mathbf{p}(s)), \\ \partial_s \mathbf{p}(s) = \nabla_{\mathbf{x}} H(s, \mathbf{z}^*(s), \mathbf{p}(s)), \\ \mathbf{z}^*(t) = \mathbf{x}, \quad \mathbf{p}(T) = \nabla_{\mathbf{x}} G(\mathbf{z}^*(T)), \\ \mathbf{u}^*(s) = \mathbf{u}^*(s, \mathbf{z}^*(s), \mathbf{p}(s)). \end{cases} \quad (6)$$

The HJB PDE, also known as the *dynamic programming* equation, corresponding to (3) is given by

$$-\partial_t \Phi(t, \mathbf{x}) + H(t, \mathbf{x}, \nabla \Phi(t, \mathbf{x})) = 0, \quad \Phi(T, \mathbf{x}) = G(\mathbf{x}) \quad (7)$$

for $(t, \mathbf{x}) \in [0, T] \times \mathbb{R}^d$, where ∇ is the gradient with respect to the state variables only. The cornerstone of the HJB approach is that the value function Φ is the unique viscosity solution of (7). Moreover, \mathbf{p} in (6) and Φ are related by

$$\mathbf{p}(s) = \nabla \Phi(s, \mathbf{z}^*(s)), \quad t < s \leq T. \quad (8)$$

Thus, the optimal control \mathbf{u}^* is given in a feedback form

$$\mathbf{u}^*(s) = \mathbf{u}^*(s, \mathbf{z}^*(s), \nabla \Phi(s, \mathbf{z}^*(s))), \quad t < s \leq T, \quad (9)$$

and \mathbf{z}^* evolves according to

$$\begin{cases} \partial_s \mathbf{z}^*(s) = -\nabla_{\mathbf{p}} H(s, \mathbf{z}^*(s), \nabla \Phi(s, \mathbf{z}^*(s))) \\ \mathbf{z}^*(t) = \mathbf{x}. \end{cases} \quad (10)$$

III. A MACHINE LEARNING APPROACH

We derive a machine learning formulation of (3) by leveraging the advantages of both the PMP and the HJB approaches. In particular, we directly optimize (2) subject to (1). Rather than solving for the controls, we first postulate the dependence of (\mathbf{z}, \mathbf{u}) on Φ according to (9), (10) and parameterize Φ by an NN. We also add penalizers that punish deviations from (7), similar to [14], [16].

A. Main formulation

Denote the control variable corresponding to initial position $\mathbf{x} \in \mathbb{R}^d$ at time $t=0$ by $\mathbf{u}_{\mathbf{x}}: [0, T] \rightarrow U$. And denote the trajectory corresponding to initial data $(0, \mathbf{x})$ by $\mathbf{z}_{\mathbf{x}}$; i.e.,

$$\partial_s \mathbf{z}_{\mathbf{x}}(s) = f(s, \mathbf{z}_{\mathbf{x}}(s), \mathbf{u}_{\mathbf{x}}(s)), \quad 0 \leq s \leq T, \quad \mathbf{z}_{\mathbf{x}}(0) = \mathbf{x}.$$

Furthermore, fix a $\rho_0 \in \mathcal{P}(\mathbb{R}^d)$ and consider the problem

$$\inf_{\{\mathbf{u}_{\mathbf{x}}\}} \int_{\mathbb{R}^d} J_{\mathbf{x}, 0}[\mathbf{u}_{\mathbf{x}}] \rho_0(\mathbf{x}) d\mathbf{x} = \inf_{\{\mathbf{u}_{\mathbf{x}}\}} \mathbb{E}_{\mathbf{x} \sim \rho_0} J_{\mathbf{x}, 0}[\mathbf{u}_{\mathbf{x}}]. \quad (11)$$

Note that $\{\mathbf{u}_x^*\}$ is a solution of (11) if and only if \mathbf{u}_x^* is an optimal control for ρ_0 a.e. $\mathbf{x} \in \mathbb{R}^d$. Thus, solving (3) with initial points \mathbf{x} in some domain Ω is equivalent to solving (11) for $\rho_0 \in \mathcal{P}(\mathbb{R}^d)$ such that $\text{supp}(\rho_0) = \Omega$. Formulation (11) is employed in mean-field game systems [14], [15] and in stabilization problems [23].

Postulating (9), (10), we arrive at our main formulation

$$\begin{aligned} & \inf_{\Phi} \mathbb{E}_{\mathbf{x} \sim \rho_0} \left(G(\mathbf{z}_x(T)) + \int_0^T L(s, \mathbf{z}_x(s), \mathbf{u}_x(s)) ds \right) \\ & \text{s.t.} \begin{cases} \mathbf{u}_x(s) = \mathbf{u}^*(s, \mathbf{z}_x(s), \nabla \Phi(s, \mathbf{z}_x(s))) \\ \partial_s \mathbf{z}_x(s) = -\nabla_{\mathbf{p}} H(s, \mathbf{z}_x(s), \nabla \Phi(s, \mathbf{z}_x(s))) \\ \mathbf{z}_x(0) = \mathbf{x}. \end{cases} \end{aligned} \quad (12)$$

We approximate Φ by an NN, $\Phi(\cdot; \theta)$, and turn (12) into a finite-dimensional optimization over the weights θ . For brevity, we often omit the explicit dependence of Φ on θ .

B. Adding HJB penalizers

We introduce three penalty terms $c_{\text{HJt}, \mathbf{x}}$, $c_{\text{HJfin}, \mathbf{x}}$, and $c_{\text{HJgrad}, \mathbf{x}}$ derived from the HJB PDE (7) as follows:

$$\begin{aligned} c_{\text{HJt}, \mathbf{x}}(t) &= \int_0^t \left| \partial_t \Phi(s, \mathbf{z}_x(s)) - H(s, \mathbf{z}_x(s), \nabla \Phi(s, \mathbf{z}_x(s))) \right| ds \\ c_{\text{HJfin}, \mathbf{x}} &= |\Phi(T, \mathbf{z}_x(T)) - G(\mathbf{z}_x(T))| \\ c_{\text{HJgrad}, \mathbf{x}} &= |\nabla \Phi(T, \mathbf{z}_x(T)) - \nabla G(\mathbf{z}_x(T))|. \end{aligned} \quad (13)$$

Penalizers prove helpful in problems similar to (12) [14], [15], [16], [24]. These penalizers improve the training convergence (Sec. III-C) without altering the solution of (12).

Adding $c_{\text{HJt}, \mathbf{x}}$, $c_{\text{HJfin}, \mathbf{x}}$, $c_{\text{HJgrad}, \mathbf{x}}$ to (12) and rewriting the time-integral in terms of ODE constraints, we obtain

$$\begin{aligned} \min_{\Phi} \mathbb{E}_{\mathbf{x} \sim \rho_0} \left(\ell_x(T) + G(\mathbf{z}_x(T)) + \alpha_1 c_{\text{HJt}, \mathbf{x}}(T) \right. \\ \left. + \alpha_2 c_{\text{HJfin}, \mathbf{x}} + \alpha_3 c_{\text{HJgrad}, \mathbf{x}} \right), \end{aligned} \quad (14)$$

subject to

$$\partial_s \begin{pmatrix} \mathbf{z}_x(s) \\ \ell_x(s) \\ c_{\text{HJt}, \mathbf{x}}(s) \end{pmatrix} = \begin{pmatrix} -\nabla_{\mathbf{p}} H(s, \mathbf{z}_x(s), \nabla \Phi(s, \mathbf{z}_x(s))) \\ L_x(s) \\ R_x(s) \end{pmatrix}, \quad (15)$$

initialized with $\mathbf{z}_x(0) = \mathbf{x}$ and $\ell_x(0) = c_{\text{HJt}, \mathbf{x}}(0) = 0$, and

$$\begin{aligned} L_x(s) &= \nabla \Phi(s, \mathbf{z}_x(s)) \cdot \nabla_{\mathbf{p}} H(s, \mathbf{z}_x(s), \nabla \Phi(s, \mathbf{z}_x(s))) \\ &\quad - H(s, \mathbf{z}_x(s), \nabla \Phi(s, \mathbf{z}_x(s))) \\ R_x(s) &= |\partial_t \Phi(s, \mathbf{z}_x(s)) - H(s, \mathbf{z}_x(s), \nabla \Phi(s, \mathbf{z}_x(s)))|. \end{aligned}$$

We note that reformulating the Lagrangian $L_x(s)$ uses (5).

The objective function thus contains the accumulated running cost $\ell_x(T)$, the HJB penalty along the trajectories $c_{\text{HJt}, \mathbf{x}}(T)$, the final-time HJB penalty $c_{\text{HJfin}, \mathbf{x}}$, and the transversality penalty $c_{\text{HJgrad}, \mathbf{x}}$. The penalty multipliers $\alpha_1, \alpha_2, \alpha_3 > 0$ are hyperparameters of the model (Sec. IV).

In each OC problem, we set up and solve (14), where f , L , and thus H vary with the problem. The L contains terms that reflect the features of the problem (Sec. III-D).

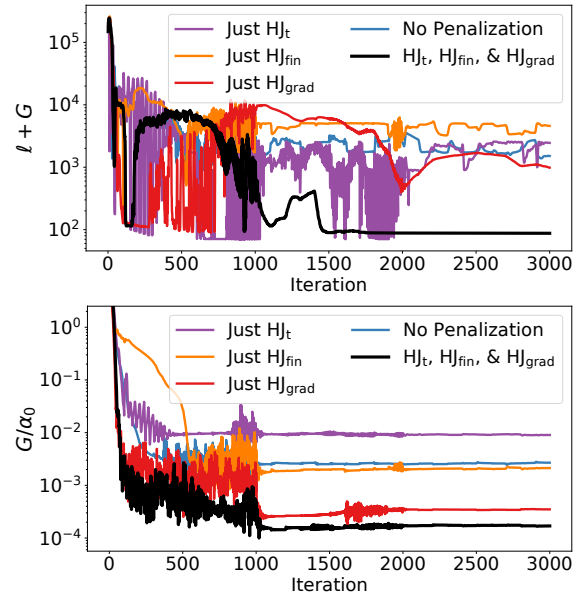


Fig. 1: We compare the validation values for models trained with different penalizers. Using all three HJB penalizers leads to the quickest convergence and the lowest G value. Each curve is the average of three training instances.

C. The effect of the HJB penalizers

We experimentally assess the effectiveness of the penalizers c_{HJt} , c_{HJfin} , c_{HJgrad} . To this end, we define nine models (all combinations of the three HJB penalizers and one with weight decay) and train each on the corridor problem (Sec. V-B). The combination of all three HJB penalizers results in the best model performance on a hold-out validation set. For brevity, we present the most relevant five of these (Fig. 1).

HJ_t: We enforce the PDE (7) describing the time derivative of Φ along the trajectories. Including this penalizer improves regularity and reduces the necessary number of time steps when solving the dynamics [25], [14], [15], [16].

HJ_{fin}: We enforce the final-time condition of the PDE (7). The inclusion of this penalizer helps the network achieve the target [14]. We observe this experimentally, where using HJ_{fin} correlates with a lower G value (Fig. 1).

HJ_{grad}: We enforce the transversality condition $\nabla \Phi(T, \mathbf{z}(T)) = \nabla G(\mathbf{z}(T))$, $\forall \mathbf{z}$, a consequence of the final-time HJB condition (7). Numerically, all conditions are enforced on a finite sample set. Therefore, higher-order regularization may help the generalization; i.e., achieving a better match of $\Phi(T, \cdot)$ and G for samples not used during training (the hold-out validation set). We observe the latter experimentally; using HJ_{grad} instead of HJ_{fin} results in better validation convergence (Fig. 1). [21] similarly enforces the values of $\nabla \Phi$.

D. Lagrangian for Obstacle and Collision Avoidance

For multi-agent problems, the Lagrangian consists of three terms: an energy term $E: \mathbb{R}^d \times U \rightarrow \mathbb{R}$ penalizing how much the agents travel, an obstacle term $Q: \mathbb{R}^d \times U \rightarrow \mathbb{R}$ penalizing agents at certain spatial locations (i.e., a terrain function),

and an interaction term $W: \mathbb{R}^d \times U \rightarrow \mathbb{R}$ penalizing the proximity among agents (i.e, collision avoidance).

We denote the state at time t for initial state \mathbf{x} by

$$\mathbf{z}_x(t) = (z_1(t), z_2(t), \dots, z_n(t)), \quad (16)$$

where $z_i \in \mathbb{R}^q$ is the state of the i th agent and $\mathbf{z} \in \mathbb{R}^d$ with $d = q \cdot n$ is the joint-state. We omit the agents' \mathbf{x} notation for brevity. Similarly, we represent the control as

$$\mathbf{u}_x(t) = (u_1(t), u_2(t), \dots, u_n(t)). \quad (17)$$

As a result, we define the Lagrangian as

$$\begin{aligned} L(\mathbf{z}_x(t), \mathbf{u}_x(t)) &= E(\mathbf{z}_x(t), \mathbf{u}_x(t)) + \alpha_4 Q(\mathbf{z}_x(t), \mathbf{u}_x(t)) \\ &\quad + \alpha_5 W(\mathbf{z}_x(t), \mathbf{u}_x(t)) \\ &= \frac{1}{n} \sum_{i=1}^n E_i(z_i(t), u_i(t)) + \frac{\alpha_4}{n} \sum_{i=1}^n Q_i(z_i(t), u_i(t)) \\ &\quad + \frac{\alpha_5}{n} \sum_{j \neq i} W_{ij}(z_i(t), z_j(t)). \end{aligned} \quad (18)$$

In this framework, the dimensionality is proportional to the number of agents. The scalars α_4, α_5 calibrate the magnitude (relative to the energy term) of the penalization of the obstacle and interactions, respectively.

IV. IMPLEMENTATION

We parameterize the value function as

$$\begin{aligned} \Phi(\mathbf{s}; \boldsymbol{\theta}) &= \mathbf{w}^\top N(\mathbf{s}; \boldsymbol{\theta}_N) + \frac{1}{2} \mathbf{s}^\top (\mathbf{A}^\top \mathbf{A}) \mathbf{s} + \mathbf{b}^\top \mathbf{s} + c, \quad (19) \\ \text{where } \boldsymbol{\theta} &= (\mathbf{w}, \boldsymbol{\theta}_N, \mathbf{A}, \mathbf{b}, c). \end{aligned}$$

Here, $\mathbf{s} = (\mathbf{x}, t) \in \mathbb{R}^{d+1}$ are the inputs corresponding to space-time, $N(\mathbf{s}; \boldsymbol{\theta}_N): \mathbb{R}^{d+1} \rightarrow \mathbb{R}^m$ is an NN, chosen as a simple two-layer residual neural network (ResNet) [26] in our experiments, and $\boldsymbol{\theta}$ contains the trainable weights: $\mathbf{w} \in \mathbb{R}^m$, $\boldsymbol{\theta}_N \in \mathbb{R}^p$, $\mathbf{A} \in \mathbb{R}^{r \times (d+1)}$, $\mathbf{b} \in \mathbb{R}^{d+1}$, $c \in \mathbb{R}$, where $\text{rank } r = \min(10, d)$ limits the number of parameters in $\mathbf{A}^\top \mathbf{A}$. Here, \mathbf{A} , \mathbf{b} , and c model quadratic potentials, i.e., linear dynamics; N models the nonlinear dynamics. We use the Python implementation of Φ and $\nabla \Phi$ described in [16].

We solve the ODE-constrained optimization problem (14) using the discretize-then-optimize approach [27], [28], in which we define a discretization of the ODE, then optimize on that discretization. The forward pass of the model uses a Runge-Kutta 4 integrator with n_t time steps to approximate the constraints (15). The objective function is then computed, and automatic differentiation [29] calculates the gradient of the objective function with respect to $\boldsymbol{\theta}$. We use the ADAM optimizer [30], a gradient-based stochastic subgradient method with momentum, to update the parameters $\boldsymbol{\theta}$. We iterate this process a selected maximum number of times. For the *learning rate* (step size) provided to ADAM, we follow a piece-wise constant decay schedule. For instance, in the corridor problem, we divide the learning rate by a factor of 10 every 1,000 iterations (Fig. 1).

The number of time steps n_t is selected *a priori* as a model hyperparameter. Large n_t leads to high computation and training time while reducing error; meanwhile, too small n_t

leads to overfitting to a refinement of the time discretization of the trajectories. To check for overfitting, we use more time steps for the hold-out validation set. For the corridor problem (Sec. V-B), we use $n_t=20$ for training and $n_t=50$ for validation (Fig. 2a). For the swarm problem (Sec. V-D), we use $n_t=26$ for training and $n_t=80$ for validation (Fig. 3). Training on a single NVIDIA Quadro RTX 8000 GPU requires about ten minutes for the corridor problem ($d=4$) and less than one hour for the swarm problem ($d=150$).

Other hyperparameters include the number of ResNet layers (tuned to equal 2), width of the ResNet m , and the multipliers $\alpha_1, \alpha_2, \alpha_3$. In contrast, some multipliers are inherent to the OC problem—e.g., $\alpha_0, \alpha_4, \alpha_5$ —and are used for both the baseline and NN.

V. NUMERICAL EXPERIMENTS

A. Baseline: Discrete Optimization for a Single Initial State

For comparison, we provide a local solution method that solves the optimal control problem for a fixed initial state $\mathbf{z}^{(0)} = \mathbf{x}_0$. To this end, we obtain a discrete optimization problem by applying forward Euler to the state equation and a midpoint rule to the integrals, which leads to

$$\begin{aligned} \min_{\{\mathbf{u}^{(k)}\}} \quad & G(\mathbf{z}^{(n_t)}) + h \sum_{k=0}^{n_t-1} L(\mathbf{s}^{(k)}, \mathbf{z}^{(k)}, \mathbf{u}^{(k)}) \quad (20) \\ \text{s.t.} \quad & \mathbf{z}^{(k+1)} = \mathbf{z}^{(k)} + h f(\mathbf{s}^{(k)}, \mathbf{z}^{(k)}, \mathbf{u}^{(k)}), \end{aligned}$$

where $h=T/n_t$. We use $T=1$ and $n_t=50$ and solve (20) using standard nonlinear programming techniques.

B. Corridor Problem

We design a four-dimensional problem in which two agents attempt to reach fixed targets on the other side of two hills. Suppose the agents with radius $r=0.5$ start at $x_1=[-2, -2]^\top$ and $x_2=[2, -2]^\top$ with targets $y_1=[2, 2]^\top$ and $y_2=[-2, 2]^\top$. Thus, the initial and target joint-states are $\mathbf{x}_0=[-2, -2, 2, -2]^\top$ and $\mathbf{y}=[2, 2, -2, 2]^\top$, respectively. We sample from ρ_0 , which is a Gaussian centered at \mathbf{x}_0 with an identity covariance. These sampled initial positions form the training set \mathbf{X} . We sample again to create the validation set.

The obstacles are defined by the spatio-temporal cost function Q_i , which we define in this experiment as the sum of four Gaussians. The energy terms are given by

$$E_i(z_i(t), u_i(t)) = \frac{1}{2} \|u_i(t)\|^2, \quad (21)$$

and the dynamics are given by $f(t, \mathbf{x}, \mathbf{u}) = \mathbf{u}$; the controls are the velocities. To model interactions for agents with radius r , we choose

$$W_{ij}(z_i, z_j) = \begin{cases} \exp\left(-\frac{\|z_i - z_j\|_2^2}{2r^2}\right), & \|z_i - z_j\|_2 < 2r \\ 0, & \text{otherwise.} \end{cases} \quad (22)$$

For terminal costs, we choose

$$G(\mathbf{z}_x(T)) = \frac{\alpha_0}{2} \|\mathbf{z}_x(T) - \mathbf{y}\|^2. \quad (23)$$

We select multipliers $\alpha_0=100$, $\alpha_4=10,000$, and $\alpha_5=300$.

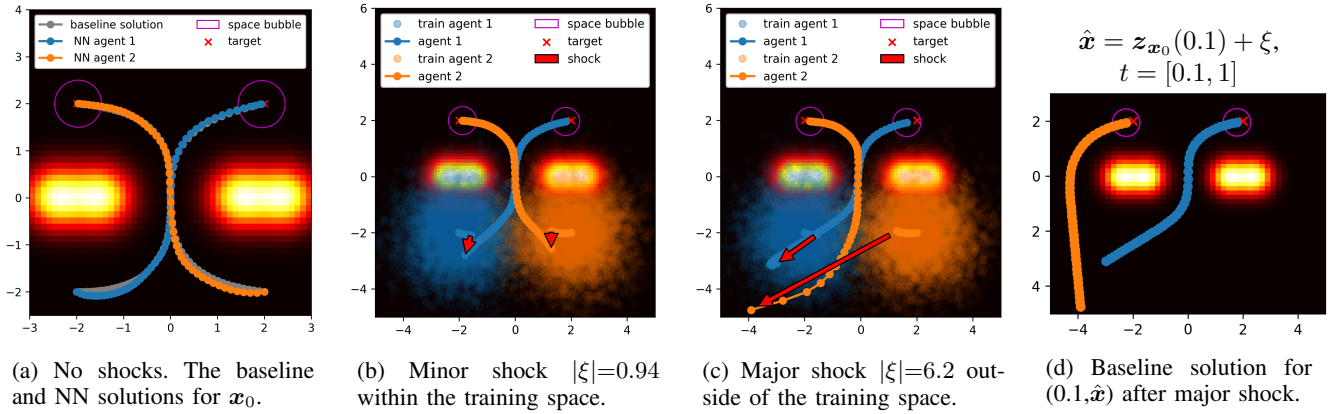


Fig. 2: Corridor problem. The NN handles a shock ξ at time $t=0.1$ (depicted with red arrows) along the trajectory. Accompanying videos are available at <https://imgur.com/a/HWq1Iot>.

TABLE I: Comparison for single instance \mathbf{x}_0 .

Scenario	Method	$\ell + G$	ℓ	G
no shocks $t \in [0, 1]$	NN	62.17	61.94	0.24
	Baseline	62.33	61.89	0.44
after shock $ \xi = 0.94$ $t \in [0.1, 1]$	NN	60.54	60.34	0.20
	Baseline	59.79	59.46	0.33
after shock $ \xi = 6.2$ $t \in [0.1, 1]$	NN	151.67	150.63	1.03
	Baseline	71.77	71.22	0.55

The baseline and the NN solve the problem with comparable trajectories (Fig. 2a) and accuracy (Table I). The NN achieves a marginally worse ℓ value but slightly better G value (Table I). We attribute the G improvement to the final-time HJB penalizers (Fig. 1).

C. Shocks

We observe that approximating the value function leads to a shock-robust model. Since the controls are in the feedback form $\partial_s z = -\nabla_p H(s, z, \nabla \Phi(s, z))$, the model can quickly calculate updated trajectories despite shocks to the system. As an example, we consider a shock ξ (implemented as a random shift) to the system at time $t=0.1$ when solving the corridor problem for $t \in [0, T]$ (Fig. 2).

Our method is designed to handle minor shocks that stay within the space of trajectories of the initial cloud about \mathbf{x}_0 . Our model computes a trajectory to \mathbf{y} for many initial points. Therefore, for point $\tilde{\mathbf{x}} \in \mathbf{X}$, the model provides dynamics $f(t, \tilde{\mathbf{x}}(t), \mathbf{u}_{\tilde{\mathbf{x}}}(t))$ before the shock. After the shock, the state picks up the trajectory of some other point $\hat{\mathbf{x}} \in \mathbf{X}$ and follows that trajectory to \mathbf{y} (Fig. 2b). In this scenario, the total trajectory has two portions

$$z_{\tilde{\mathbf{x}}}(0.1) = \int_0^{0.1} f(t, z_{\tilde{\mathbf{x}}}(t), \mathbf{u}_{\tilde{\mathbf{x}}}(t)) dt, \quad z_{\tilde{\mathbf{x}}}(0) = \tilde{\mathbf{x}}, \quad \text{and}$$

$$z_{\hat{\mathbf{x}}}(1) = \int_{0.1}^1 f(t, z_{\hat{\mathbf{x}}}(t), \mathbf{u}_{\hat{\mathbf{x}}}(t)) dt, \quad z_{\hat{\mathbf{x}}}(0.1) = z_{\tilde{\mathbf{x}}}(0.1) + \xi,$$

before and after the shock, respectively. We imagine a minor shock then as moving from one trajectory to another

(Fig. 2b). The results of the control problem along $t=[0.1, 1]$ for the NN and baseline solutions are similar (Table I).

Interestingly, our model extends outside the training region (Fig. 2c). Although the vast majority of NNs cannot extrapolate, our NN still solves the control problem after a major shock, demonstrating some extrapolation capabilities. We note that the NN solves the original problem for \mathbf{x}_0 to near optimality. However, after such a large shock, the NN solves the control problem, but with little hope for optimality. In our example, we compare the NN's solution (Fig. 2c) with the baseline's solution for $t=[0.1, 1]$ (Fig. 2d). The NN learned a solution in which agent 2 passes through the corridor followed by agent 1. After the major shock, the NN still applies these dynamics (Fig. 2c) while the baseline finds a more optimal solution (Fig. 2d). The NN is roughly 50% less optimal (Table I).

We attribute the shock robustness to the NN parameterization of the global value function. Experimentally, the shock robustness of our model (Fig. 2) does not noticeably differ from a model trained without penalization. Since the NN is trained prior and offline, it handles shocks in real-time. In contrast, methods that solve for a single trajectory—e.g., the baseline—must pause to recompute following a shock.

D. Swarm Trajectory Planning

We demonstrate the high-dimensional capabilities of our model by solving a swarm trajectory planning problem in the spirit of [22]. The swarm problem contains 50 three-dimensional agents that fly from initial to target positions while avoiding each other and obstacles. We construct Q_i to model rectangular prism obstacles and use (21), (22), and (23) for energy, interaction, and terminal costs. The NN learns to guide all agents around the obstacles (Fig. 3). Naturally, if the time discretization is too coarse (small n_t), then the model may simulate collisions solely due to inaccurate time integration. In validation, we see that the agents avoid the obstacles and each other by observing values for Q and W are exactly 0.

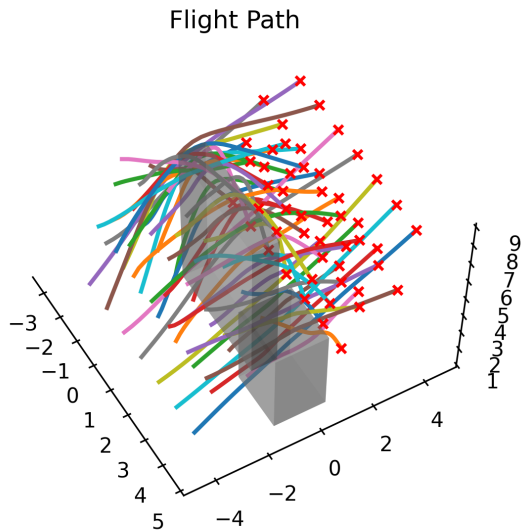


Fig. 3: Swarm Trajectory Planning for 50 agents in \mathbb{R}^3 .

VI. CONCLUSION AND OUTLOOK

We formulate and demonstrate an efficient NN approach for solving high-dimensional OC problems. Our method aims at computing the optimal control in feedback form in the relevant subset of the space-time domain. It combines the high-dimensional scalability from PMP and the global nature from HJB approaches. Using a numerical example, we demonstrate that the obtained feedback form generalizes outside the training space, which allows the agents to react to unforeseen events such as shocks. Our future endeavors relate to further experimentation of our method on OC problems with more involved dynamics.

REFERENCES

- [1] W. H. Fleming and H. M. Soner, *Controlled Markov processes and viscosity solutions*, 2nd ed., ser. Stochastic Modelling and Applied Probability. Springer, New York, 2006, vol. 25.
- [2] M. Bardi and I. Capuzzo-Dolcetta, *Optimal control and viscosity solutions of Hamilton-Jacobi-Bellman equations*, ser. Systems & Control: Foundations & Applications. Birkhäuser Boston, Inc., Boston, MA, 1997, with appendices by Maurizio Falcone and Pierpaolo Soravia.
- [3] P. Cannarsa and C. Sinestrari, *Semiconcave functions, Hamilton-Jacobi equations, and optimal control*, ser. Progress in Nonlinear Differential Equations and their Applications. Birkhäuser Boston, Inc., Boston, MA, 2004, vol. 58.
- [4] L. S. Pontryagin, V. G. Boltyanskii, R. V. Gamkrelidze, and E. F. Mishchenko, *The mathematical theory of optimal processes*, ser. Translated by K. N. Tririgoff; edited by L. W. Neustadt. Interscience Publishers John Wiley & Sons, Inc. New York-London, 1962.
- [5] R. Bellman, *Dynamic programming*. Princeton University Press, Princeton, N. J., 1957.
- [6] W. Kang and L. C. Wilcox, “Mitigating the curse of dimensionality: sparse grid characteristics method for optimal feedback control and HJB equations,” *Computational Optimization and Applications*, vol. 68, no. 2, pp. 289–315, 2017.
- [7] W. Kang, Q. Gong, and T. Nakamura-Zimmerer, “Algorithms of data development for deep learning and feedback design,” *arXiv:1912.00492*, 2019.
- [8] B. Rivière, W. Hönl, Y. Yue, and S.-J. Chung, “Glas: Global-to-local safe autonomy synthesis for multi-robot motion planning with end-to-end learning,” *IEEE Robotics and Automation Letters*, vol. 5, no. 3, pp. 4249–4256, 2020.

- [9] A. T. Lin, Y. T. Chow, and S. J. Osher, “A splitting method for overcoming the curse of dimensionality in Hamilton–Jacobi equations arising from nonlinear optimal control and differential games with applications to trajectory generation,” *Communications in Mathematical Sciences*, vol. 16, no. 7, pp. 1933–1973, 2018.
- [10] J. Darbon and S. Osher, “Algorithms for overcoming the curse of dimensionality for certain Hamilton–Jacobi equations arising in control theory and elsewhere,” *Research in the Mathematical Sciences*, vol. 3, no. 1, p. 19, 2016.
- [11] M. R. Kirchner, R. Mar, G. Hewer, J. Darbon, S. Osher, and Y. T. Chow, “Time-optimal collaborative guidance using the generalized Hopf formula,” *IEEE Control Systems Letters*, vol. 2, no. 2, pp. 201–206, 2018.
- [12] M. R. Kirchner, G. Hewer, J. Darbon, and S. Osher, “A primal-dual method for optimal control and trajectory generation in high-dimensional systems,” *2018 IEEE Conference on Control Technology and Applications (CCTA)*, pp. 1583–1590, 2018.
- [13] S. Osher and C.-W. Shu, “High-order essentially nonoscillatory schemes for Hamilton–Jacobi equations,” *SIAM Journal on numerical analysis*, vol. 28, no. 4, pp. 907–922, 1991.
- [14] L. Ruthotto, S. J. Osher, W. Li, L. Nurbekyan, and S. W. Fung, “A machine learning framework for solving high-dimensional mean field game and mean field control problems,” *Proceedings of the National Academy of Sciences (PNAS)*, vol. 117, no. 17, pp. 9183–9193, 2020.
- [15] A. T. Lin, S. W. Fung, W. Li, L. Nurbekyan, and S. J. Osher, “APACnet: Alternating the population and agent control via two neural networks to solve high-dimensional stochastic mean field games,” *arXiv:2002.10113*, 2020.
- [16] D. Onken, S. W. Fung, X. Li, and L. Ruthotto, “OT-Flow: Fast and accurate continuous normalizing flows via optimal transport,” *arXiv:2006.00104*, 2020.
- [17] J. Han and W. E, “Deep learning approximation for stochastic control problems,” 2016.
- [18] W. E, J. Han, and A. Jentzen, “Deep learning-based numerical methods for high-dimensional parabolic partial differential equations and backward stochastic differential equations,” *Communications in Mathematics and Statistics*, vol. 5, no. 4, pp. 349–380, Nov 2017.
- [19] J. Han, A. Jentzen, and W. E, “Solving high-dimensional partial differential equations using deep learning,” *Proceedings of the National Academy of Sciences*, vol. 115, no. 34, pp. 8505–8510, Aug 2018.
- [20] N. Nüsken and L. Richter, “Solving high-dimensional Hamilton-Jacobi-Bellman PDEs using neural networks: perspectives from the theory of controlled diffusions and measures on path space,” *arXiv:2005.05409*, 2020.
- [21] T. Nakamura-Zimmerer, Q. Gong, and W. Kang, “Adaptive deep learning for high dimensional Hamilton-Jacobi-Bellman equations,” *arXiv:1907.05317*, 2019.
- [22] W. Hönl, J. A. Preiss, T. S. Kumar, G. S. Sukhatme, and N. Ayanian, “Trajectory planning for quadrotor swarms,” *IEEE Transactions on Robotics*, vol. 34, no. 4, pp. 856–869, 2018.
- [23] K. Kunisch and D. Walter, “Semiglobal optimal feedback stabilization of autonomous systems via deep neural network approximation,” *arXiv:2002.08625*, 2020.
- [24] C. Finlay, J.-H. Jacobsen, L. Nurbekyan, and A. M. Oberman, “How to train your neural ODE: the world of Jacobian and kinetic regularization,” 2020.
- [25] L. Yang and G. E. Karniadakis, “Potential flow generator with L_2 optimal transport regularity for generative models,” *arXiv:1908.11462*, 2019.
- [26] K. He, X. Zhang, S. Ren, and J. Sun, “Deep residual learning for image recognition,” in *IEEE Conference on Computer Vision and Pattern Recognition (CVPR)*, 2016, pp. 770–778.
- [27] A. Gholaminejad, K. Keutzer, and G. Biros, “ANODE: Unconditionally accurate memory-efficient gradients for neural ODEs,” in *International Joint Conference on Artificial Intelligence (IJCAI)*, 2019, pp. 730–736.
- [28] D. Onken and L. Ruthotto, “Discretize-optimize vs. optimize-discretize for time-series regression and continuous normalizing flows,” *arXiv:2005.13420*, 2020.
- [29] J. Nocedal and S. Wright, *Numerical optimization*. Springer Science & Business Media, 2006.
- [30] D. P. Kingma and J. Ba, “Adam: A method for stochastic optimization,” in *International Conference on Learning Representations (ICLR)*, 2015.